Pagination not final/Pagination non finale

Vol. 49, No. 3, September 2003 Vol. 49, no 3, septembre 2003

Evaluation of Control Implementation in Real-Time Simulation of an Aircraft Landing Approach

Hugh H.T. Liu * William D. Harman *

Abstract

Modern robust flight-control techniques often result in sophisticated control laws that require a high level of computing power. The implementation and affordability must be addressed for practical reasons. Evaluation of the controller design can best be achieved, perhaps, through real-time simulation. In this paper, we present a real-time control and simulation investigation in an aircraft-landing example, as one test-case study. The control law is required to be stability robust with respect to variations in speed, weight, centre-of-gravity position, time delays, and tolerant to failures. Focus is placed upon control-law implementation and performance evaluation in real-time simulation. The results give rise to practical considerations when evaluating and selecting the control laws. A further comparison and rating analysis suggest a quantitative sensitivity criterion of real-time application. The purpose of this investigation is to take into account the computational capabilities in flight-control applications, as an effort to bring the sophisticated design one step closer to practice.

continued on page 2

* Institute for Aerospace Studies
University of Toronto
4925 Dufferin Street
Toronto, ON M3H 5T6, Canada.
E-mail: liu@utias.utoronto.ca

Received 10 February 2003.

Nomenclature

p	roll rate in body-fixed frame FB (rad/s)
q	pitch rate in FB (rad/s)
r	yaw rate in FB (rad/s)
u_B	x-component of the inertial velocity in FB (m/s)
u_V	x-component of the inertial velocity in vehicle-carried frame FV (m/s)
v_B	y-component of the inertial velocity in FB (m/s)
v_V	y-component of the inertial velocity in FV (m/s)
w_B	z-component of the inertial velocity in FB (m/s)
w_V	z-component of the inertial velocity in FV (m/s)
α	angle of attach (rad)
β	angle of sideslip (rad)
δ_A	aileron control input (rad)
δ_e	elevator control input (rad)
δ_R	rudder control input (rad)
δ_{TH}	throttle control input (rad)
θ	pitch angle (Euler angle) (rad)
ϕ	roll angle (Euler angle) (rad)
ψ	heading angle (Euler angle) (rad)

1. Introduction

The development of an autopilot is a demanding task when the aircraft dynamics is affected by various kinds of uncertainties, such as an atmospheric disturbance, a fault/failure situation, a dynamic model inaccuracy, or unmodelled characteristics. Research into the flight-control robustness to such uncertainties has progressed and developed many design approaches, including, for example, linear-quadratic (LQ) methods; eigenstructure assignment (EA); slide-mode control; adaptive control, H_∞; μ-synthesis; and nonlinear approaches such as feedback linearization, dynamic inversion, Lyapunov methods, and so on. Generally speaking, modern robust control techniques tend to result in highly sophisticated control and decision-making algorithms, and evaluation of these different control laws can best be achieved, perhaps, through real-time simulation.

The final decision of control selection depends not only on their contribution to performance improvement, but also on their implementation and affordability (Wise, 1995). In other

PROOF/ÉPREUVE

suite de la page 1

Résumé

Les techniques de commande de vol modernes robustes engendrent souvent des lois de pilotage évoluées qui nécessitent une grande puissance de calcul. Pour des raisons pratiques, il faut se pencher sur leur mise en oeuvre et leur abordabilité. L'évaluation de la conception du dispositif de pilotage peut sans doute être mieux réalisée au moyen de la simulation en temps réel. Dans le document, nous présentons l'étude de la simulation et du pilotage en temps réel d'un atterrissage comme étude de cas. La loi de pilotage doit être robuste en stabilité par rapport aux variations de vitesse, de masse, de centrage, de délais, et elle doit tolérer des défaillances. L'accent est mis sur la mise en oeuvre de la loi de pilotage et l'évaluation de la performance dans le cadre d'une simulation en temps réel. Les résultats suscitent des considérations pratiques lorsqu'il s'agit de sélectionner et d'évaluer des lois de pilotage. Une analyse de comparaison et de classification plus poussée permet de dégager un critère de sensibilité quantitative relativement à une application en temps réel. La présente étude vise à prendre en compte les capacités de calcul dans les applications relatives aux commandes de vol afin de rapprocher une conception évoluée de la pratique.

words, flight computer and computational capabilities must be addressed for control approach selection (Chamitoff, 1993). In this paper, we present a real-time control and simulation investigation in an aircraft-landing example, as one test case study. Extensive research work has been carried out on this example with respect to robust flight-control design and evaluation, which is summarized in Magni et al. (1997). A brief description will also be given later in Sect. 2. The contribution of this paper focuses on control-law implementation and performance evaluation under a real-time simulation environment. The results give rise to practical considerations when evaluating and selecting the control laws. A further analysis suggests a quantitative sensitivity criterion. The purpose of this investigation is to take into account the computational capabilities in flight control applications, in an effort to bring the sophisticated design one step closer to practice.

The remainder of this paper is organized as follows. In Sect. 2, the benchmark aircraft is briefly described, followed by introduction of several control-law candidates (Sect. 3) and testing criteria (Sect. 4). In Sect. 5, the real-time simulation results are presented. Afterwards, the detailed analysis and discussions are provided in Sect. 6. Finally, the concluding remarks are offered in Sect. 7.

2. An Aircraft-Landing Example

A robust flight-control design benchmark was defined by the Group for Aeronautical Research and Technology in Europe (GARTEUR). The objective was to assess the applicability of modern robust control-design concepts to flight-control problems (GARTEUR, 1997). One of the two benchmark models, the Research Civil Aircraft Model (RCAM), addresses the design of an autopilot for the final approach of a transport airplane, after an engine failure occurs. The control law is required to be stability robust with respect to variations in speed, weight, centre-of-gravity (CG) position, time delays, nonlinearity, engine failure, and the presence of gusts of wind. The flight mission of the landing approach is shown in **Figure 1**.

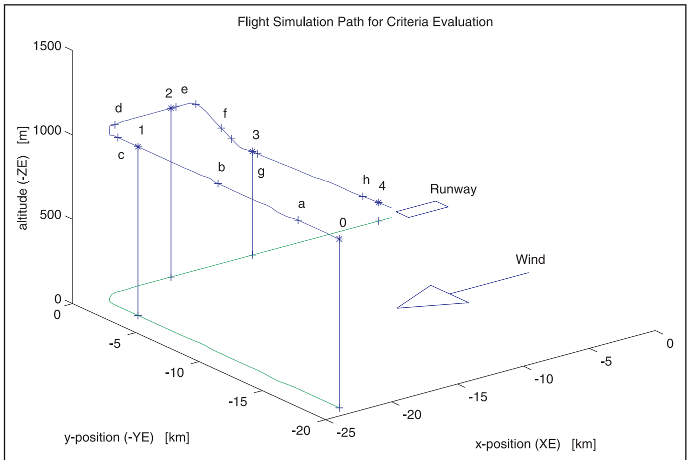

Figure 1. Testing Flight Mission: A Landing Approach. Engine Failure Appears at Point a.

The flight path is divided into four segments.

- Segment I (point 0 to point 1). Starting at an altitude of 1000 m, a level flight is to be maintained with a constant airspeed of 80 m/s. During this level flight, an engine failure occurs at point a and the engine restarts at point b.
- Segment II (point 1 to point 2). This segment consists of a commanded-coordinated turn from point c to point d to maintain the constant speed and the lateral acceleration close to zero.
- Segment III (point 2 to point 3). The descent phase starts with a $\gamma = -6°$ approach at point e, and a descent with $\gamma = -3°$ at point f.
- Segment IV (point 3 to point 4). The glide slope of $\gamma = -3°$ is to be maintained during a wind shear between points g and h.

This benchmark aircraft model and its landing approach was deemed ideal for our investigation, since its complexity poses a reasonable challenge for control implementation and real-time simulation.

3. Controller Implementation

Three different robust flight control techniques were chosen to implement for real-time control and simulation. Each of these controllers originally was the design submission to the GARTEUER RCAM challenge. These three design approaches are the normalized coprime factorization method with loop shaping (NCFLS) (GARTEUR, 1995); the eigenstructure assignment (EA) (de la Cruz et al., 1997); and the Lyapunov method (LYA) (Daafouz et al., 1997). The controller is divided into longitudinal and lateral components that are treated separately. Each is broken down further into inner and outer loops. The purpose of the inner loop is to stabilize and augment the handling qualities of the aircraft while the outer loop guides the aircraft along the generated trajectory. It is also assumed that all signals are perfect.

Take the NCFLS controller as an example. The longitudinal channel consists of four states (q, θ, u_B, w_B), two inputs (δ_e and δ_{TH}), and three outputs (q, V, and w_V). The measurement (feedback) signals used by the longitudinal inner loop are: pitch rate, velocity, and vertical velocity. The outer loop is responsible for altitude tracking and thus uses altitude as its feedback signal. The lateral controller is designed in a similar fashion to the longitudinal one. The lateral controller consists of five states (p, r, ϕ, ψ, and v_B), two inputs (δ_A and δ_R), and six outputs (β, p, r, ϕ, and v_V). The lateral inner loop makes use of the roll angle and the sideslip angle as feedback signals while the outer loop uses a sideslip integrator for reducing sideslip during asymmetric flight cases (e.g., engine 1 failure).

Implementation of the controllers involves re-modelling the RCAM model into a modular graphical block diagram structure, developed on the Matlab/Simulink and RT_Lab, a real-time simulation platform (Opal-RT, 2000). Detailed modelling efforts are reported in Harman and Liu (2002a). Further, implementation of the EA controller are presented in Harman and Liu (2002b). **Figures 2** and **3** show the Simulink block diagram structure of the longitudinal and lateral NCFLS controller, respectively. The overall system block diagram is shown in **Figure 4**.

4. Test Criteria

The designed controller is to be evaluated by the following criteria to "obtain an objective comparison between completely different controllers" at each phase: P, performance; S, safety; Q, quality; C, control; and R, robustness. Further, four (4) different test cases are considered to represent variations: (i) the nominal case; (ii) the CG fwd case where the horizontal centre of gravity has been shifted to the most forward position; (iii) the CG aft case where the CG is shifted to the most afterward position; and (iv) the time-delay case where the flight is executed with a nominal centre of gravity and a time delay of 100 ms. In this paper, values of criteria P, Q, C, and S are taken as the average of the four-test-case results, while the stability robustness R algorithm is calculated based on all four test cases, unless otherwise specified.

Quantitative evaluation criteria for each Segment was originally reported in GARTEUR (1997) and also presented in Harman and Liu (2002b) with modification. For completeness, the criteria for each segment are presented in the Appendix. According to the calculation formula, the smaller the values are, the better the performance they represent.

5. Real-Time Simulation Results

The real-time simulation was conducted on a real-time systems simulator (RTSS), at the Laboratory of Flight Systems and Control, the University of Toronto Institute for Aerospace Studies (FSC-UTIAS). The RTSS consists of a networked cluster of high-end commercial off-the-shelf (COTS) real-time computers with hardware-in-the-loop capabilities, and is suitable for our proposed distributed and real-time simulation of the benchmark aircraft model (Liu, 2001). The current equipment setup is depicted in **Figure 5**.

Detailed real-time simulation results for using the EA controller are reported in Harman and Liu (2002b). In this paper, we first present the simulation results for using the NCFLS controller, then a complete list of simulation results from all three controllers is presented.

5.1. NCFLS Controller Results

The controller implemented here is the NCFLS-designed control law. The real-time simulation is conducted on the RTSS with a sampling time of 0.01 s.

Segment I defines a lateral deviation boundary of 20 m to account for the effect of turbulence, and a boundary of 100 m during engine failure. The real-time simulation result in **Figure 6**, shows that the NCFLS controller is unable to maintain the aircraft within the specified lateral deviation boundaries during the engine failure and restart. While this implies that a re-design of the controller is necessary, using alternative design methods (Harman and Liu, 2002b), this sub-standard controller configuration will be retained for the rest of this paper for comparison purposes.

The objectives at Segment II are to maintain a constant speed of 80 m/s, to keep the lateral acceleration close to zero, to restrict the bank angle to $\phi = 30°$ with consistent rudder/aileron deflections, but not to exceed a lateral deviation of 200 m during the entire segment, and not to exceed a lateral deviation of 20 m at the end of Segment II. The real-time simulation results are shown in **Figures 7** and **8**. It is demonstrated that the trajectory of the model surpasses the bounds but the lateral deviation never exceeds the maximum value of 200 m and at the end the lateral deviation is close to zero.

The real-time simulation results of Segment III are shown in **Figures 9** and **10**. Both figures represent the behaviour of the model in the descent phase. They shown that the trajectories of the model surpass the bounds although the vertical deviation

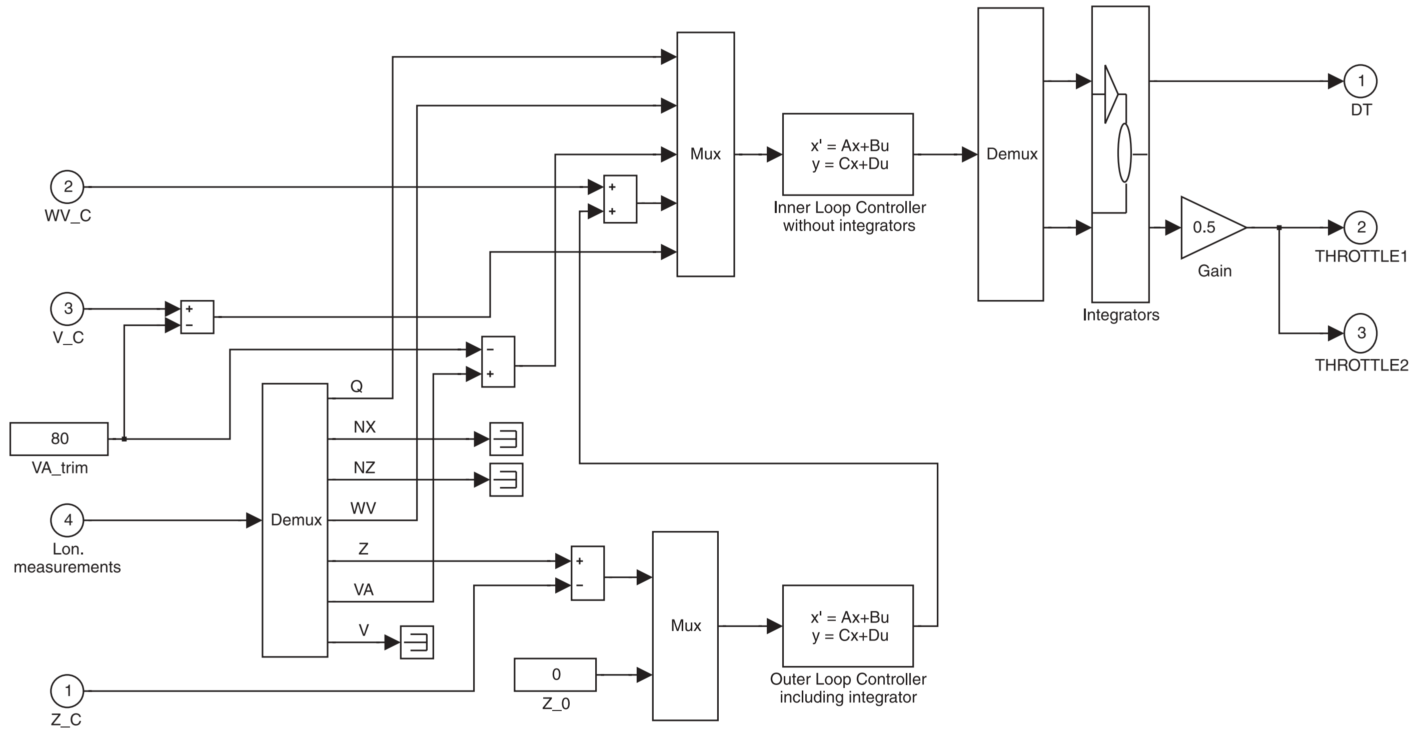

Figure 2. Structure of the Longitudinal NCFLS Controller.

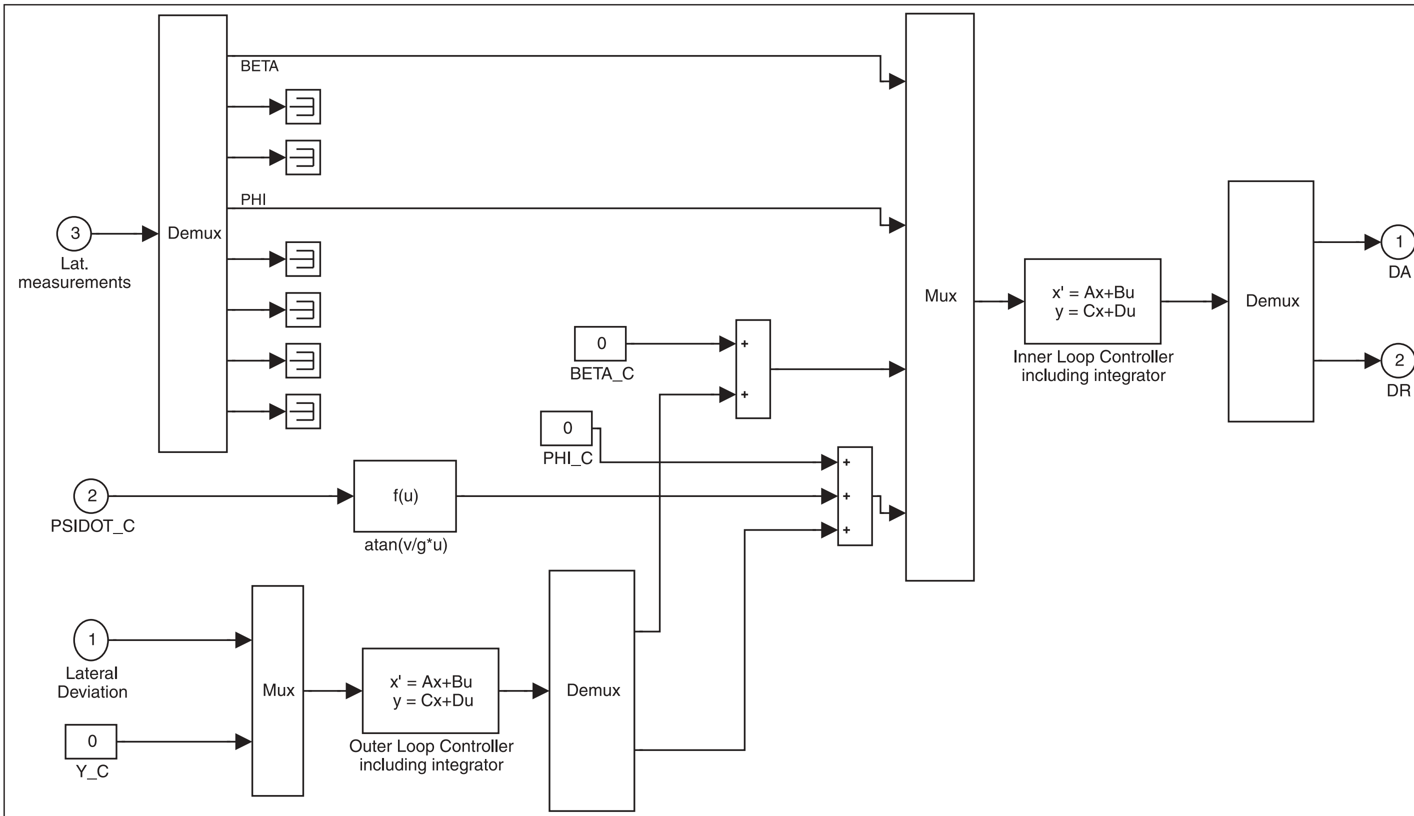

Figure 3. Structure of the Lateral NCFLS Controller.

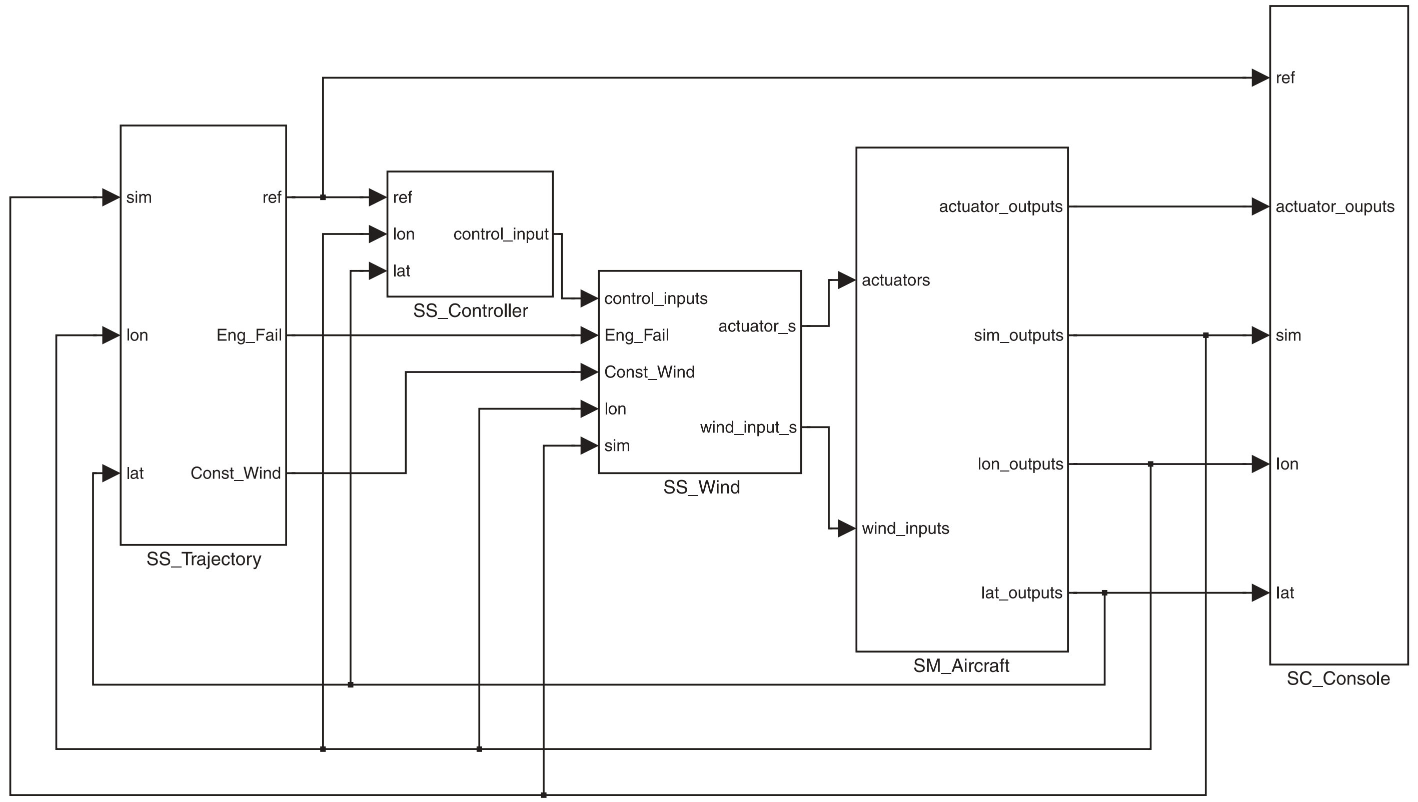

Figure 4. RCAM System Block Diagram.

never exceeds the maximum value of 20 m and at the end of Segment III the deviation is close to zero.

During the final approach, as shown in **Figures 11** and **12** for Segment IV, a maximum deviation of 20 m should not be exceeded, and at its end a maximum deviation of 1.5 m is taken into account. It can be seen that the trajectories of the model fall inside the bounds during the entire segment. The rest of the specifications are also fulfilled.

The robustness criterion for each segment sets the limits of maximal allowable deviations and the limit at the end of each segment, under all four test cases representing different kinds of variations. The numerical measures of evaluation of all four segments are listed in **Table 1**.

5.2. Complete Results of All Three Controllers

The complete real-time simulation results, of all three controllers (i.e., NCFLS-, EA-, and LYA-designed control laws) are listed in **Table 2**. The simulator keeps the same 100 Hz rate for all three candidates. The values are taken as an average of all four test cases, except for the stability robustness R.

6. Evaluation Analysis

6.1. NRT versus RT of NCFLS Controller

The real-time (RT) simulation results are further compared with off-line (non- real-time, or NRT) simulation results. The comparison results of the NCFLS controller application are presented in **Figures 13–16**. The numerical values are listed in **Tables 3–6**. At the nominal configuration, the differences between RT and NRT results are negligible. The values for the maximum-time-delay configuration do exhibit some minor differences. However, it is worth pointing out the differences in the numerical treatment of NRT and RT simulations. NRT simulations perform calculation after calculation, with no regard for time constraints, at the fastest speed available until the simulation is complete. In RT, the incorporation of hard-time constraints express how critical every fraction of a second is. By incorporating a time delay between the controller outputs and actuator inputs, in RT, certain instances of data logging could be delayed or ultimately omitted if not performed within the FSS. Whereas in NRT, no concern for time constraints ensures that all events take place and are logged in sequence.

In summary, we conclude that for one controller (the NCFLS controller in this example), the numerical values of the evaluation measures are not significantly different for the non-real-time versus the real-time implementation. These minor differences indicate that he sampling rate and time-delay effects that are implemented differently in the real-time versus non-real-time simulation and the computational approaches used in the real-time implementation of this controller to meet the hard-time requirements are acceptable.

6.2. Evaluation of Three Controllers

The most interesting observation, out of our real-time control and simulation investigation, is the sensitivity of the

Figure 5. UTIAS RTSS Facility.

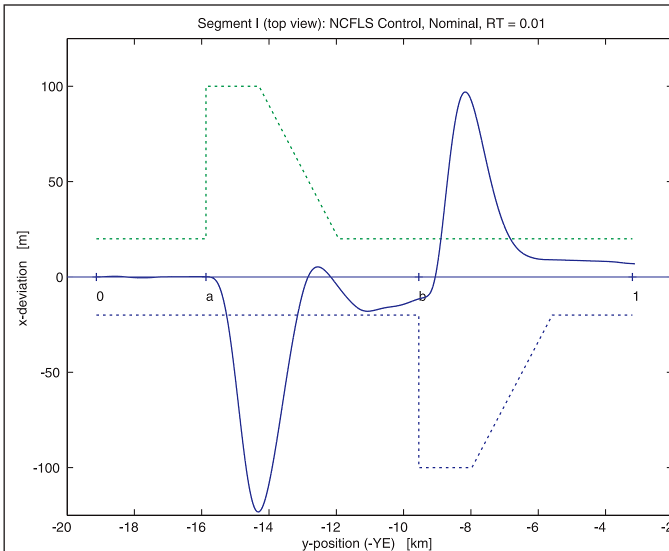

Figure 6. Segment I Real-Time Simulation Results, RT = 0.01 s, with broken lines showing the boundary.

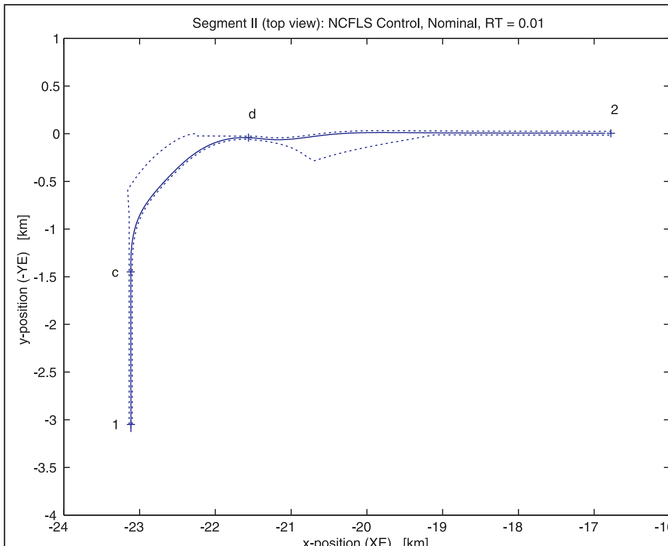

Figure 7. Segment II Real-Time Simulation Results, RT = 0.01 s, with broken lines showing the boundary.

controller implementation to the testing criteria preservation. At the previous subsection, the relative error between NRT and RT results is formulated as the deviation between the two

$$\text{Error} = \frac{|RT - NRT|}{|NRT|} \times 100\% \qquad (1)$$

When this formula is applied to all the test results of the three controllers, we found that the NCFLS controller committed an average deviation of 1.7005%, the LYA controller accounted for a 1.369% deviation, however, the EA controller ended up with a 4.535% deviation.

Further, we came up with a rating scheme to compare criteria values obtained from different controllers. For each criterion, we normalize the maximum value of the three results giving it a value of 1, and the other two are given a relative ratio. For example, in the criterion of P_1 of **Table 2**, the maximum value of max (0.7898, 0.0768, 0.1754) is achieved when the NCFLS controller is applied. As a result, the rating of the NCFLS controller on P_1 is 1.0, the rating of the EA controller is 0.0768/0.7898 = 0.10, and the rating of the LYA controller becomes 0.22. Taking the total of all the ratings that each controller received from all evaluation criteria, we find the rating of the NCFLS controller is 15.55, the rating of the EA controller is 9.34, and the rating of the LYA controller is 14.71.

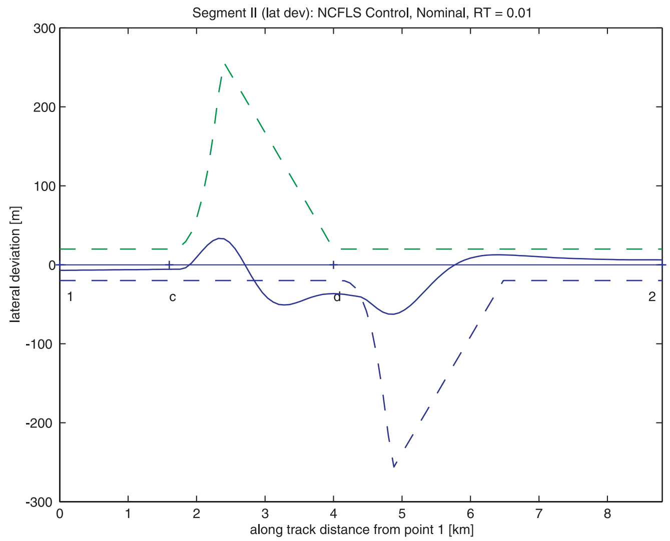

Figure 8. Segment II Real-Time Simulation Results, RT = 0.01 s, with broken lines showing the boundary.

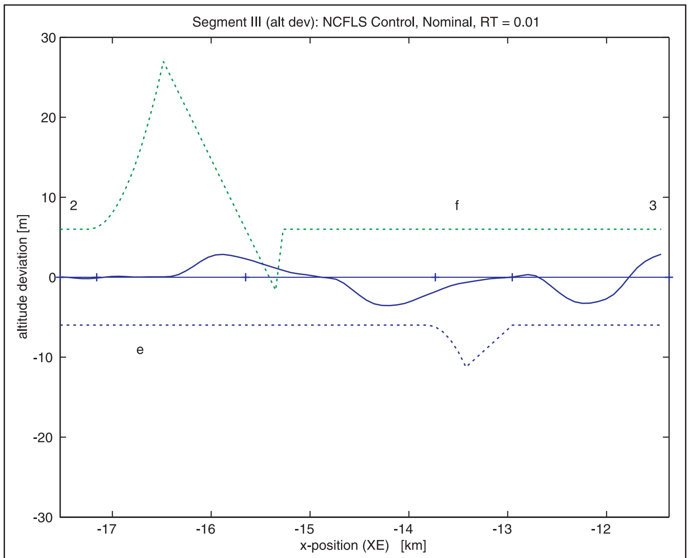

Figure 10. Segment III Real-Time Simulation Results, RT = 0.01 s, with broken lines showing the boundary.

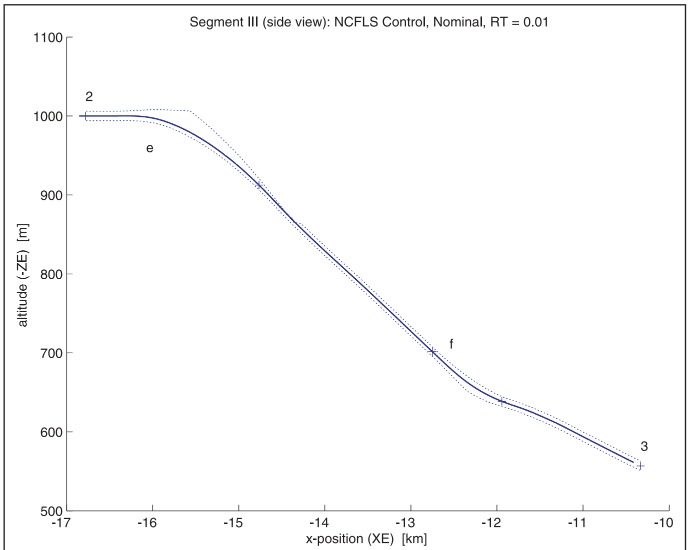

Figure 9. Segment III Real-Time Simulation Results, RT = 0.01 s, with broken lines showing the boundary.

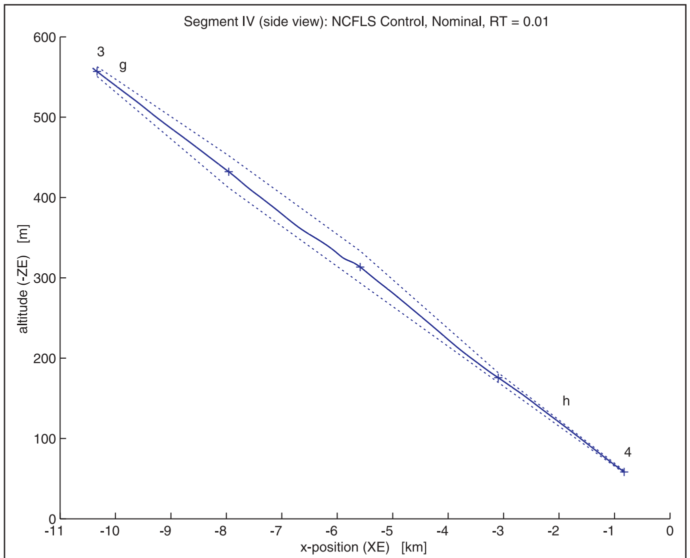

Figure 11. Segment IV Real-Time Simulation Results, RT = 0.01 s, with broken lines showing the boundary.

Assuming that the smaller the value of the criteria the better the performance, the conclusion seems to be consistent with the NRT comparison, where the EA controller delivers the best result. On the other hand, however, if we compare the ratings of all three controllers from their NRT results, we found that the EA controller is much more sensitive to the real-time implementation than the other two, as shown in **Table 7**.

In summary, we conclude that even though the EA controller still delivers better results than the other two, both in NRT and RT cases, one needs to consider the sensitivity before final selection is made. Our simulation results suggest the possibility that a controller is designed to satisfaction in the NRT environment, but the performance may degrade when it is implemented for a real-time application. Further, its sensitivity to the sampling-rate, time delay may cause serious concerns. It gives rise to some practical considerations at the implementation stage of sophisticated control laws.

7. Conclusions

Robust flight-control techniques often result in sophisticated control laws. Their promising features need to be evaluated in a real-time simulation. The controller implementation and real-time simulation investigation on a benchmark aircraft on its landing approach, presented in this paper, demonstrated that design and evaluation must be addressed, taking into account the computational capabilities. The sensitivity study gives rise

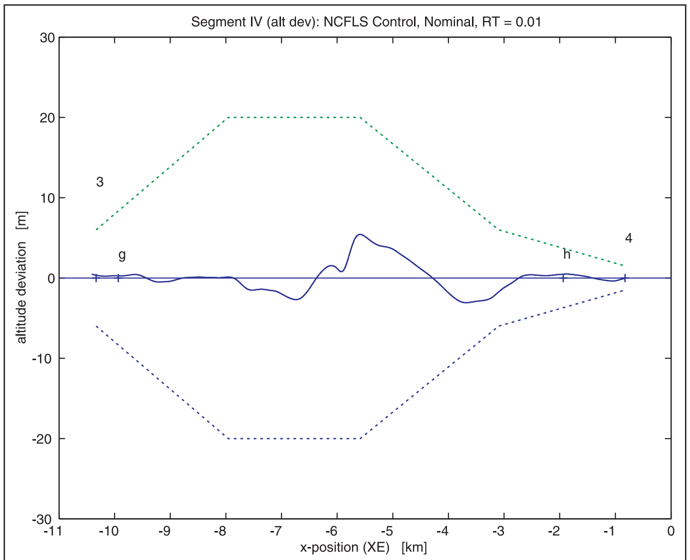

Figure 12. Segment IV Real-Time Simulation Results, RT = 0.01 s, with broken lines showing the boundary.

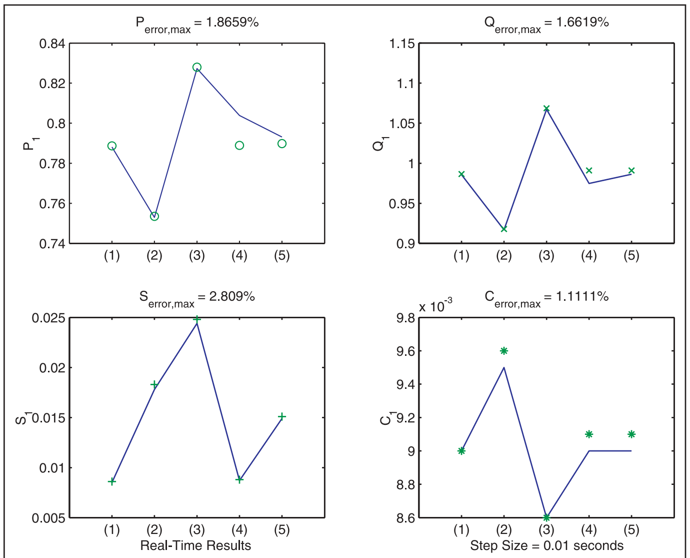

Figure 13. Segment I Criteria Evaluation: Symbols, RT; Line, NRT. Case: (1), Nominal; (2), CG Fwd; (3), CG Aft; (4), Delay; (5), Average.

Table 1. Numerical Results of the Real-Time Simulation (*P, Q, S, C* in the Nominal Case).

Segment	*P*	*Q*	*S*	*C*	*R*
I	0.7887	0.9866	0.0086	0.0090	0.4539
II	0.2872	1.3574	0.1215	0.0082	0.1961
III	0.1030	1.4204	0.0093	0.0160	0.7607
IV	0.1499	0.7205	0.0526	0.0319	0.4102
Average	0.3322	1.1212	0.0480	0.0163	0.4552

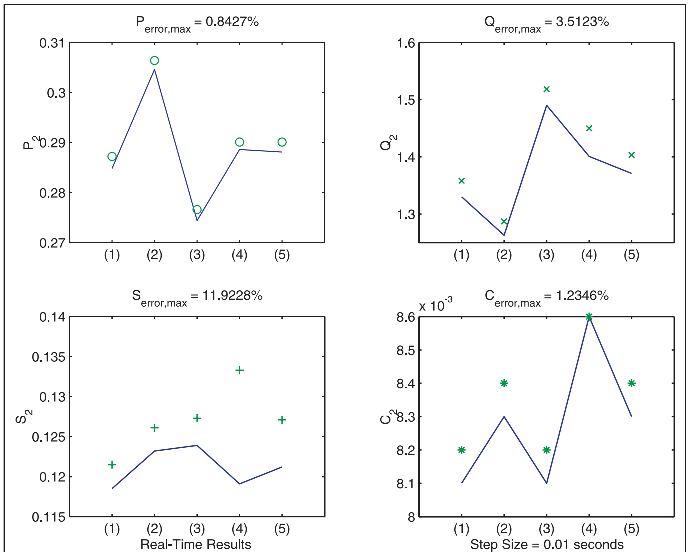

Figure 14. Segment II Criteria Evaluation: Symbols, RT; Line, NRT. Case: (1), Nominal; (2), CG Fwd; (3), CG Aft; (4), Delay; (5), Average.

Table 2. Complete Real-Time Simulation Results: RT = 0.01 s.

Segment/criteria (Average)	NCFLS	EA	LYA
P_1	0.7898	0.0768	0.1754
Q_1	0.9910	0.5506	0.5084
S_1	0.0151	0.0070	0.0100
C_1	0.0091	0.0032	0.0047
R_1	0.4539	0.0320	0.0814
P_2	0.2901	0.6096	0.1101
Q_2	1.4033	0.7134	17.1588
S_2	0.1271	0.0306	0.1665
C_2	0.0084	0.0025	0.0233
R_2	0.1961	0.0149	0.3538
P_3	0.1015	0.3495	0.6155
Q_3	1.4494	1.1910	1.3967
S_3	0.0096	0.0081	0.0059
C_3	0.0166	0.0166	0.0155
R_3	0.7607	0.5036	0.1574
P_4	0.1723	0.1974	0.2238
Q_4	0.7439	0.6191	0.6455
S_4	0.0621	0.0382	0.1105
C_4	0.0325	0.0325	0.0294
R_4	0.4102	0.1705	0.4805

to practical considerations before the control law is adopted for implementation and application. The overall evaluation of the control techniques must be conducted in both non- real-time and real-time simulations. A quantitative rating criterion may serve as a valuable tool for the sensitivity study.

The sensitivity itself, in RT simulation, may be affected by several factors, such as the sampling rate, time delay, complexity of the control laws, the method of modelling, and the efficiency of the algorithms. That leaves a possible topic for future study. Further, it would be worthwhile studying digital-control design to account for implementation directly. It is an on-going effort at our research group. Findings and results may be reported in the future.

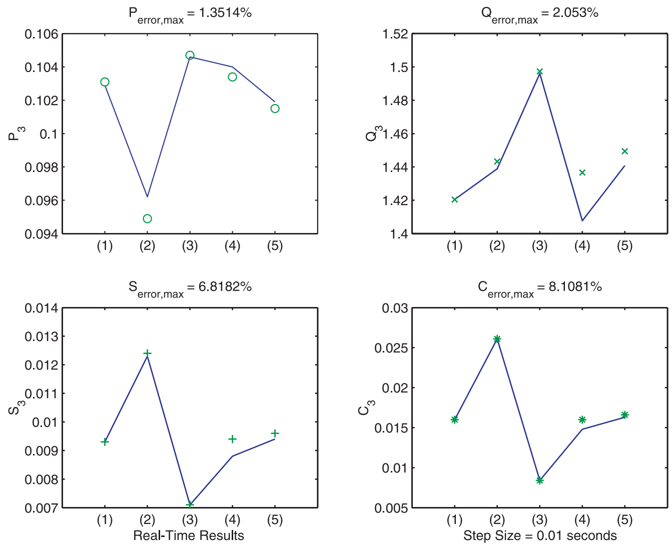

Figure 15. Segment III Criteria Evaluation: Symbols, RT; Line, NRT. Case: (1), Nominal; (2), CG Fwd; (3), CG Aft; (4), Delay, (5), Average.

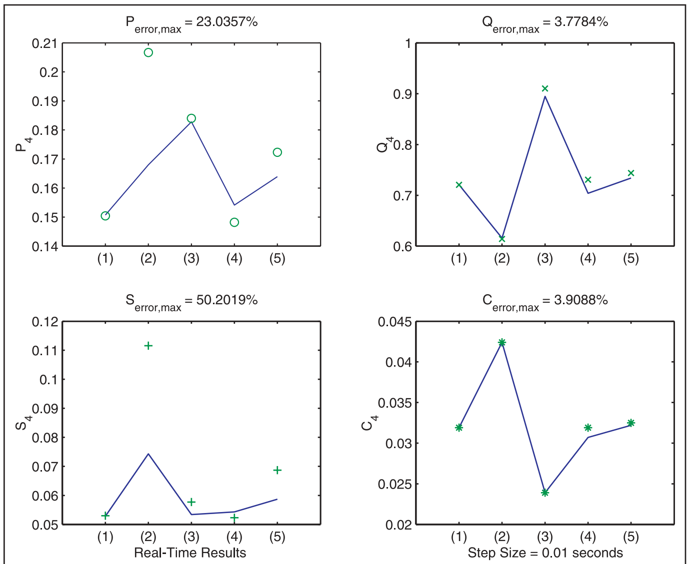

Figure 16. Segment IV Criteria Evaluation: Symbols, RT; Line, NRT. Case: (1), Nominal; (2), CG Fwd; (3), CG Aft; (4), Delay; (5), Average.

References

Chamitoff, G.E. (1993). "The Application of Intelligent Search Strategies to Robust Flight Control of Hypersonic Vehicles". AIAA Tech. Rep., No. 93-3732-CP.

Daafouz, J., Arzelier, D., Garcia, G., and Bernussou, J. (1997). "RCAM Design Challenge Presentation Document: The Lyapunov Approach". Tech. Rep. TP-088-14, Group for Aeronautical Research and Technology in Europe (GARTEUR), Action Group FM (AG08).

de la Cruz, J., Ruiperez, P., and Aranda, J. (1997). "RCAM Design Challenge Presentation Document: An Eigenstructure Assignment Approach". Tech. Rep. TP-088-22, Group for Aeronautical Research and Technology in Europe (GARTEUR), Action Group FM (AG08).

Table 3. Segment I Real-Time (RT) and Non- Real-Time (NRT) Measurement Comparison.

Segment I	NRT	RT	Error (%)
P_1			
Nominal	0.7881	0.7887	0.0761
CG fwd	0.7530	0.7535	0.0664
CG aft	0.8273	0.8280	0.0846
Time delay	0.8039	0.7889	1.8659
Average	0.7931	0.7898	0.4161
Q_1			
Nominal	0.9857	0.9866	0.0913
CG fwd	0.9169	0.9178	0.0982
CG aft	1.0672	1.0686	0.1312
Time delay	0.9748	0.9910	1.6619
Average	0.9862	0.9910	0.4867
S_1			
Nominal	0.0085	0.0086	1.1765
CG fwd	0.0178	0.0183	2.8090
CG aft	0.0244	0.0248	1.6393
Time delay	0.0087	0.0088	1.1494
Average	0.0149	0.0151	1.3423
C_1			
Nominal	0.0090	0.0090	0.0000
CG fwd	0.0095	0.0096	1.0526
CG aft	0.0086	0.0086	0.0000
Time delay	0.0090	0.0091	1.1111
Average	0.0090	0.0091	1.1111

Table 4. Segment II Real-Time (RT) and Non-Real-Time (NRT) Measurement Comparison.

Segment II	NRT	RT	Error (%)
P_2			
Nominal	0.2848	0.2872	0.8427
CG fwd	0.3046	0.3064	0.5909
CG aft	0.2744	0.2766	0.8017
Time delay	0.2886	0.2901	0.5198
Average	0.2881	0.2901	0.6942
Q_2			
Nominal	1.3301	1.3582	2.1126
CG fwd	1.2629	1.2869	1.9004
CG aft	1.4900	1.5182	1.8926
Time delay	1.4008	1.4500	3.5123
Average	1.3710	1.4033	2.3559
S_2			
Nominal	0.1185	0.1215	2.5316
CG fwd	0.1232	0.1261	2.3539
CG aft	0.1239	0.1273	2.7441
Time delay	0.1191	0.1333	11.9228
Average	0.1212	0.1271	4.8680
C_2			
Nominal	0.0081	0.0082	1.2346
CG fwd	0.0083	0.0084	1.2048
CG aft	0.0081	0.0082	1.2346
Time delay	0.0086	0.0086	0.0000
Average	0.0083	0.0084	1.2048

Table 5. Segment III Real-Time (RT) and Non-Real-Time (NRT) Measurement Comparison.

Segment III	NRT	RT	Error (%)
P_3			
Nominal	0.1029	0.1031	0.1944
CG fwd	0.0962	0.0949	1.3514
CG aft	0.1046	0.1047	0.0956
Time delay	0.1040	0.1034	0.5769
Average	0.1019	0.1015	0.3925
Q_3			
Nominal	1.4205	1.4204	0.0070
CG fwd	1.4389	1.4433	0.3058
CG aft	1.4960	1.4973	0.0869
Time delay	1.4077	1.4366	2.0530
Average	1.4408	1.4494	0.5969
S_3			
Nominal	0.0093	0.0093	0.0000
CG fwd	0.0123	0.0124	0.8130
CG aft	0.0071	0.0071	0.0000
Time delay	0.0088	0.0094	6.8182
Average	0.0094	0.0096	2.1277
C_3			
Nominal	0.0160	0.0160	0.0000
CG fwd	0.0261	0.0261	0.0000
CG aft	0.0084	0.0084	0.0000
Time delay	0.0148	0.0160	8.1081
Average	0.0163	0.0166	1.8405

GARTEUR. (1995). “RCAM Preliminary Design Document”. Tech. Rep. TP-088-9, Group for Aeronautical Research and Technology in Europe (GARTEUR), Action Group FM (AG08).

GARTEUR. (1997). “Robust Flight Control Design Challenge Problem Formulation and Manual: The Research Civil Aircraft Model (RCAM)”. Tech. Rep. TP-088-3, Group for Aeronautical Research and Technology in Europe (GARTEUR), Action Group FM (AG08).

Harman, D., and Liu, H. (2002a). “Robust Flight Control: A Distributed Simulation Implementation”. *Proceedings of the AIAA Modeling and Simulation Technologies Conference and Exhibit*, Monterey, California, 5–8 August 2002. American Institute of Aeronautics and Astronautics, Reston, Va. p. 4473.

Harman, D., and Liu, H. (2002b). “Robust Flight Control: A Real-Time Simulation Investigation”. *Proceedings of the 23rd International Congress of Aeronautical Sciences (ICAS)*,International Council of the Aeronautical Sciences, Reston, Va. p. 5.4.3.

Liu, H. (2001). “Real-Time System Simulation Using COTS for Flight Control Integration”. *Proceedings of the AIAA Modeling and Simulation Technologies Conference and Exhibit*, p. 4186.

Magni, J.-F., Bennani, S., and Terlouw, J. (Editors). (1997). “Robust Flight Control: A Design Challenge”, Springer-Verlag, New York.

OPAL-RT. (2000). “RT_LAB 4.2 User’s Guide”. The Opal-RT Technologies Inc.,

Wise, K.A. (1995). “Applied Controls Research Topics in the Aerospace Industry”. *Proceedings of the 34th Conference on Decision and Control*, pp. 751–755.

Table 6. Segment IV Real-Time (RT) and Non-Real-Time (NRT) Measurement Comparison.

Segment IV	NRT	RT	Error (%)
P_4			
Nominal	0.1507	0.1504	0.1991
CG fwd	0.1680	0.2067	23.0357
CG aft	0.1828	0.1840	0.6565
Time delay	0.1541	0.1482	3.8287
Average	0.1639	0.1723	0.3925
Q_4			
Nominal	0.7208	0.7205	0.0416
CG fwd	0.6158	0.6140	0.2923
CG aft	0.8948	0.9103	1.7322
Time delay	0.7040	0.7306	3.7784
Average	0.7339	0.7439	1.3626
S_4			
Nominal	0.0528	0.0530	0.3788
CG fwd	0.0743	0.1116	50.2019
CG aft	0.0534	0.0577	8.0524
Time delay	0.0543	0.0523	3.6832
Average	0.0587	0.0687	17.0358
C_4			
Nominal	0.0319	0.0319	0.0000
CG fwd	0.0424	0.0424	0.0000
CG aft	0.0239	0.0239	0.0000
Time delay	0.0307	0.0319	3.9088
Average	0.0322	0.0325	0.9317

Table 7. Rating Comparison of Three Controllers.

Controller	RT rating	NRT rating	Sensitivity (%)
NCFLS	15.55	15.57	0.13
LYA	14.71	14.75	0.27
EA	9.34	10.21	9.31

Acknowledgements

The work described in this paper was partially supported by a grant from the Natural Sciences and Engineering Research Council (NSERC) of Canada Research Grant. The experimental facility was supported by the Canada Foundation for Innovation (CFI) New Opportunities Program and Ontario Innovation Trust (OIT).

Appendix A. Testing Evaluation Criteria

A.1. Segment I

The *performance criterion* of Segment I defines the lateral deviation boundary of 20 m to account for the effect of turbulence, and the boundary of 100 m during engine failure. The *quality criterion* considers the maximum lateral acceleration of 0.2g. The *safety criterion* sets the limit of the maximum angle of attack α of 12°. The *control criterion* concerns the rudder actuator effort to stabilize the aircraft after engine failure is recovered. And the *robustness criterion* sets the limit of maximal allowable deviations and the limit at the end of this segment.

$$P_1 = \frac{1}{2}\left(\max_{t_0 \le t \le t_1} \frac{|e_{yb}(t)|}{100} + \frac{|e_{yb}(t_1)|}{20}\right) \tag{A.1}$$

$$Q_1 = \max_{t_0 \le t \le t_1}\left(\frac{|n_y(t)|}{0.2}\right) \tag{A.2}$$

$$S_1 = \max_{t_0 \le t \le t_1}\left(\frac{|\alpha(t)|}{12}\right)^3 \tag{A.3}$$

$$C_1 = \int_{t_b}^{t_1} \delta_{\mathrm{R}}^2 \,\mathrm{d}t \tag{A.4}$$

$$R_1 = \frac{1}{2}\max_{t_0 \le t \le t_1}\left(\frac{|\Delta_{eyb}(t)|}{10} + \frac{|\Delta_{eyb}(t_1)|}{2}\right) \tag{A.5}$$

where $e_{\mathrm{yb}}(t)$ denotes the lateral deviation in body coordinates.

A.2. Segment II

The *performance criterion* defines the maximum lateral deviation of 200 m due to the turn and the lateral deviation of 20 m at the end of the segment. The *quality criterion* considers the maximum lateral acceleration of 0.02g. The *safety criterion* sets the limit of the maximum angle of attack α of 12°. The *control criterion* concerns the rudder and aileron actuator effort. The *robustness criterion* sets the limit of maximal allowable lateral deviations with perturbed centre of gravity and time delays.

$$P_2 = \frac{1}{2}\left(\max_{t_1 \le t \le t_2} \frac{|e_{yb}(t)|}{200} + \frac{|e_{yb}(t_2)|}{20}\right) \tag{A.6}$$

$$Q_2 = \max_{t_1 \le t \le t_2}\left(\frac{|n_y(t)|}{0.02}\right) \tag{A.7}$$

$$S_2 = \max_{t_1 \le t \le t_2}\left(\frac{|\alpha(t)|}{12}\right)^3 \tag{A.8}$$

$$C_2 = \int_{t_1}^{t_2} \left(\delta_R^2 + \delta_A^2\right) \mathrm{d}t \tag{A.9}$$

$$R_2 = \frac{1}{2}\max_{t_1 \le t \le t_2}\left(\frac{|\Delta_{eyb}(t)|}{20} + \frac{|\Delta_{eyb}(t_2)|}{2}\right) \tag{A.10}$$

A.3. Segment III

The *performance criterion* considers the maximum vertical deviation during the capture of the –6° glide slope and the vertical deviation at the end of this segment. Further, speed variations should be kept small in spite of the change in required angle of attack. The *quality criterion* considers the maximum vertical acceleration. The *safety criterion* sets the limit of the maximum angle of attack α of 12°. The *control criterion* concerns the tailplane actuator effort. The *robustness criterion* sets the limit of maximal allowable vertical deviations with perturbed centre of gravity and time delays.

$$P_3 = \frac{1}{3}\left(\max_{t_2 \le t \le t_3} \frac{|e_{zb}(t)|}{20} + \frac{|e_{zb}(t_3)|}{6} + \max_{t_2 \le t \le t_3} \frac{|V - V_{command}|}{4}\right) \tag{A.11}$$

$$Q_3 = \max_{t_2 \le t \le t_3}\left(\frac{|n_z(t)|}{0.05}\right) \tag{A.12}$$

$$S_3 = \max_{t_2 \le t \le t_3}\left(\frac{|\alpha(t)|}{12}\right)^3 \tag{A.13}$$

$$C_3 = \int_{t_2}^{t_3} \delta_T^2 \,\mathrm{d}t \tag{A.14}$$

$$R_3 = \frac{1}{2}\max_{t_2 \le t \le t_3}\left(\frac{|\Delta_{ezb}(t)|}{2} + \frac{|\Delta_{ezb}(t_3)|}{0.6}\right) \tag{A.15}$$

A.4. Segment IV

The *performance criterion* considers the maximum vertical deviation due to the wind shear and the vertical deviation at the end of this segment. The *quality criterion* considers the maximum vertical acceleration. The *safety criterion* considers whether the aircraft is within the decision window at the end of the segment. The *control criterion* considers the tailplane and throttle actuator effort. The *robustness criterion* sets the limit of maximal allowable vertical deviations with perturbed centre of gravity and time delays.

$$P_4 = \frac{1}{2}\left(\max_{t_3 \le t \le t_4} \frac{|e_{zb}(t)|}{20} + \frac{|e_{zb}(t_4)|}{1.5}\right) \tag{A.16}$$

$$Q_4 = \max_{t_3 \le t \le t_4}\left(\frac{|n_z(t)|}{0.2}\right) \tag{A.17}$$

$$S_4 = \sqrt{\frac{1}{3}\left[\left(\frac{e_{yb}}{5}\right)^2 + \left(\frac{e_{ab}}{1.5}\right)^2 + \left(\frac{V - V_{command}}{3}\right)^2\right]} \tag{A.18}$$

$$C_4 = \int_{t_3}^{t_4} \left[\delta_T^2 + (\delta_{T_{H1}} + \delta_{T_{H2}})^2 \right] \mathrm{d}t \tag{A.19}$$

$$R_4 = \frac{1}{2} \left(\max_{t_c \le t \le t_d} \frac{|\Delta_{ezb}(t)|}{2} + \frac{|\Delta_{ezb}(t_d)|}{0.15} \right) \tag{A.20}$$